Rare Metal Materials and Engineering
Volume 48, Issue 4, April 2019
Available online at www.rmme.ac.cn

Science Press

Cite this article as: Rare Metal Materials and Engineering, 2019, 48(4): 1087-1095.

ARTICLE

Corrosion Behaviour of Arc Sprayed Zn55Al Coatings on Q235 Steel in 3.5 wt% NaCl Solution

Feng Shangbin, Jia Lina, Zhang Huarui, Wang Fangfang, Liu Guangxu, Zhang Hu

Beihang University, Beijing 100191, China

Abstract: A Zn55Al pseudo-alloy wires with high Al content were prepared by multi-core canned hot extrusion and a cold drawing method, and then they were deposited on Q235 steel by arc spraying to form a Zn55Al coating. The microstructure of the Zn55Al pseudo-alloy wire was investigated by scanning electron microscopy (SEM) and micro-region X-ray diffraction (Micro-XRD). The corrosion behaviours of the Zn55Al coating and pure Al coating as well as the Zn15Al coating were investigated by an immersion corrosion test and electrochemical measurements, and the difference between the coatings was also assessed. The results indicate that Zn55Al pseudo-alloy wires are composed of pure Zn and pure Al. An alloying phenomenon does not occur in the whole formation process. The Zn55Al coating that contains Zn-rich phases and Al-rich phases exhibits an obvious lamellar structure with a few holes and gaps. After 20 d of immersion, it is found that the Zn55Al coating forms a dense passive film and has better corrosion resistance than the Zn15Al coating. The corrosion potential (E_{corr}) of the Zn55Al coatings is approximately –1.25 V, which is more positive than that of the Zn15Al coatings but is more negative than that of the pure Al coatings and the Q235 substrate. The results of galvanic corrosion test also shows that the Zn55Al coating can provide better electrochemical protection than Zn15Al coating to the Q235 substrate. This suggests that Zn55Al coating displays not only a better corrosion resistance but also a stronger electrochemical protection to the Q235substrate. The protective mechanisms of the Zn55Al coating were also discussed.

Key words: multi-core canned hot extrusion; Zn55Al pseudo-alloy wire; Zn55Al coating; corrosion behaviour

The corrosion phenomenon of steel structures and equipment is very common in many fields. Numerous efforts have been undertaken to protect steel from corrosion[1-4]. The use of a metallic coating system, for example Zn-Al coatings, is an effective approach for avoiding steel corrosion[5-9]. Arc-sprayed Zn-Al alloy coatings are widely used as long-lasting corrosion protection for large steel workpieces because of the dramatic electrochemical protection of Zn, the excellent erosion resistance of the Al content and its high production efficiency, low production cost and flexible operation[10-12]. Zn-Al alloy coatings can be usually applied in oil industry, bridges, ships and other fields. Currently, Zn5Al and Zn15Al are the most widely used coatings, but the corrosion resistance of these coatings has been found to be significantly reduced under high humidity or high salt spray conditions. This has motivated an intense research effort for enhancing the corrosion resistance of Zn-Al coatings. Many studies have focused on the addition of Si, Mg, rare earth elements (RE) and other alloying elements into Zn-Al coatings in order to enhance their corrosion resistance[13-16].

Some studies have demonstrated that the corrosion resistance of Zn-Al coatings can be remarkably improved as the Al content increased[7,17,18]. The Zn55Al coating has better corrosion resistance than Zn15Al coating in the environment with high chloride contents[19]. Another advantage of high Al content Zn-Al coating is the reduction of the coating production cost because Al is cheaper than Zn. Therefore, the research on multicomponent Zn-Al alloy wires with a high Al

---

Received date: April 20, 2018
Foundation item: National Key Research and Development Program of China (2016YFB0300901)

Corresponding author: Jia Lina, Ph. D., School of Materials Science and Engineering, Beihang University, Beijing 100191, P. R. China, Tel: 0086-10-82316958, E-mail: jialina@buaa.edu.cn

content has evoked great interest during the last few years.

It is well-known that traditional arc-sprayed Zn-Al alloy wire is usually produced through the process of melting, casting and drawing. However, when the Al content exceeds 15%, the Zn-Al alloy wires become too hard to be drawn[16]. In recent years, several new methods were investigated for the preparation of high Al content Zn-Al wire. Yan et al successfully manufactured Zn26Al wires using the cored wires method[20]. However, the production of cored wires requires the use of high-quality zinc powder, aluminum powder and an alloy belt, leading to a high production cost and limiting their application and further development.

Multi-core canned hot extrusion and cold drawing are usually used for the preparation of superconducting wires[21-23]. Unfortunately, few studies have applied this method to the production of Zn-Al pseudo-alloy wire. In the present paper, the Zn55Al coating was prepared by arc-spraying the Zn-55Al pseudo-alloy wires. The surface morphology and the corrosion resistance of the Zn55Al coatings were investigated. The primary goal of the present paper is to prepare Zn55Al pseudo-alloy wires by following this unusual formation process and study the corrosion behaviour of the Zn55Al coating.

1 Experiment

Zn55Al pseudo-alloy wire was prepared by multi-core canned hot extrusion and drawing. As shown in Fig.1, the extrusion billet consists of an Al alloy can, some Al alloy bars and some pure Zn bars. The composite billet was extruded as a 10 mm bar by a 400 t extruder at 280~320 °C. Then, the 10 mm pseudo-alloy bar was drawn to 3 mm wires by the multiple pass drawing process. Finally, Zn55Al pseudo-alloy wires, Zn15Al wires and pure Al wires with the diameter of 3 mm were used to prepare Zn55Al coating, Zn15Al coating and pure Al coating, respectively on cold-rolled Q235 steel sheet using arc-spray equipment. The Q235 substrate was grit blasted with corundum at the pressure of approximately 0.6 MPa just prior to spraying to remove contamination from the surface and generate a roughened surface for promoting coating adhesion. Compressed air was used to remove the dust and scrap iron from the grit blasting. The coatings were developed with an arc-spraying gun and an arc-spraying machine at room temperature. The specific parameters of the arc spray are summarized in Table 1. To investigate the corrosion behaviour of the Zn-Al coating more accurately, the sealing treatment is not adapted to all the three kinds of coatings. Three kinds of coating samples were cut into 14 mm×14 mm×3 mm sections for use in electrochemical testing.

To investigate the corrosion behaviour of the coatings, the immersion corrosion test and the electrochemical measurements were adopted. All tests were carried out in a 3.5 wt% NaCl solution at room temperature. The open circuit potential-immersion time curves (E_{ocp}-t) and potentiodynamic polarization curve were obtained by a CHI660N electrochemical working station. The galvanic corrosion behaviors of Zn55Al coating and Q235 substrate, as well as Zn15Al coating and Q235 substrate were investigated. All experiments for each group were repeated three times to obtain average values and ensure the reproducibility of the experiment.

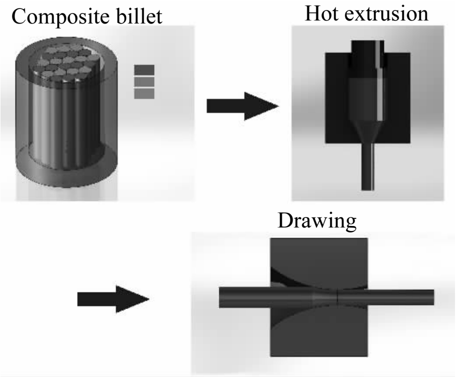

Fig.1 Formation process of the Zn55Al pseudo-alloy wire

Table 1 Spraying parameters used for Zn55Al, Zn15Al and Al coatings preparation

Spraying parameter	Value
Voltage/V	30
Current/A	130~140
Air pressure/MPa	0.6
Distance/mm	100~150

The electrochemical tests were conducted in a conventional H-type three electrolytic cell at room temperature. The saturated calomel electrode (SCE) was used as the reference electrode, and a 2 cm^2 platinum electrode was used as the auxiliary electrode. The coatings with the exposure area of 1 cm² were used as the working electrode. The potentiodynamic polarization curve was measured at the sweep rate of 0.1 mV/s in the range of ±0.6 V versus open circuit potential. The 3.5 wt% NaCl solution was refreshed daily to ensure the composition of the solution did not change. The open circuit potential (OCP) was recorded for the immersion time of 1, 3, 5, 8, 12, 24, 48, 72, 120, 168, 240, 360 and 480 h.

The galvanic corrosion experiences were carried out in the 3.5 wt% NaCl solution at room temperature. SCE was used as the reference electrode and the working area of Zn55Al coating, Zn15Al coating and Q235 substrate were 1 cm^2. The distance between two work electrodes was 4 cm. The galvanic potential (E_{g}) and the galvanic current (I_{g}) were recorded every 10 min within 6 h.

In the present work, scanning electron microscopy (SEM) was applied to observe the cross-section morphology of the Zn55Al pseudo-alloy wire, the microstructure of the coating surface, the cross-section morphology of the coating and the morphology of the corrosion products. The macroscopic corrosion morphology of the three coatings was observed using an Asana microscope. The phase composition of the Zn55Al pseudo-alloy wire and the coatings were investigated by energy dispersive spectrum analysis (EDS) and X-ray diffraction (XRD). The porosity of the Zn55Al coating was measured by a gray scale method. The Image J software was used to count the area rate of pores and gaps in the SEM images of the Zn55Al coating. 25 different SEM images were analyzed to obtain average values.

2 Results and Discussion

2.1 Characterization of Zn55Al pseudo-alloy wire

Fig.2a shows the cross-section morphology of the Zn55Al pseudo-alloy wire as displayed in the backscattered electron image (BEI) obtained by SEM. Examination of Fig.2a shows that the composite billet is deformed into a solid wire after the extrusion and drawing process. The cavity in the composite billet is filled with Zn bars and Al bars during the deformation. The thickness of Al can of the wire is approximately 0.1~0.2 mm. It is clear that Zn bars and Al bars after deformation are wrapped tightly by the pure Al can. The distribution maps of Zn element and Al element, obtained by EDS, are shown in Fig.2b and Fig.2c. The results show that Zn and Al are two separate parts after extrusion and drawing process. The shapes of Zn part and Al part depend on the arrangement of the Zn bars and the Al bars in the original belt.

The boundary between the two phases (shown by the yellow circle in Fig.2a was detected by Micro-XRD, and the result is shown in Fig.2d. The Micro-XRD results show that the Zn55Al pseudo-alloy wire is composed only of pure Zn phase and pure Al phase. As a result, the alloying phenomenon does not occur during the entire formation process. Therefore, this wire is significantly different from the traditional Zn-Al alloy wires. The hard and brittle phases generated in the cast process do not exist in the pseudo-alloy wire.

As we know, Al forms the face-centered cubic structure (fcc), whereas Zn forms the dense hexagonal structure (hcp) at room temperature. The deformation ability of Al is better than that of Zn because the fcc structure has more slip systems than the hcp structure. Therefore, pure Al can play the role of a lubricant between the Zn and the drawing die in the deformation process. Thus, the Al can and bars could improve the deformation ability of Zn bars. The composite billet was under three-dimensional compressive stress during the entire extrusion process, which can also improve the deformation capacity of Zn.

Through reasonable control of the extrusion parameters, including the extrusion temperature and the extrusion speed, the temperature of the composite does not exceed the eutectic temperature of the Zn-Al alloy. In addition, the drawing process was carried out at room temperature. The temperature of the wires is much lower than the eutectic temperature that even produced some heat during the drawing process. The Zn55Al pseudo-alloy wire is composed of pure Zn and pure Al. Therefore, the entire deformation process is the deformation of pure Al and pure Zn. There are no eutectic structures and hard and brittle phases to obstruct the deformation of the wire. Consequently, the multi-core canned hot extrusion and drawing method avoids the problem of the difficult alloy drawing due to the high Al content.

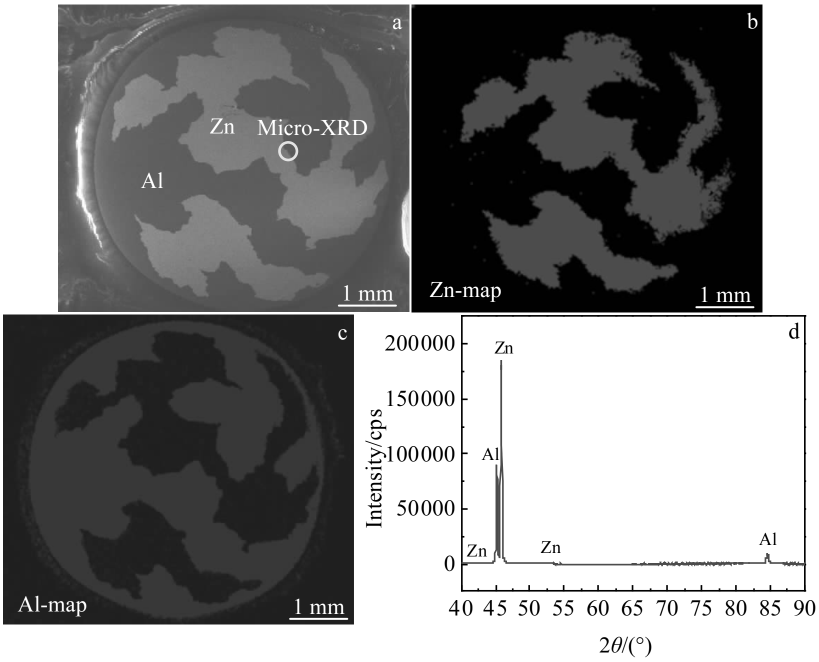

Fig.2 Cross-section morphology (BEI) of Zn55Al pseudo-alloy wire (a); distribution of Zn (b) and Al (c) elements; (d) XRD pattern of the yellow circle in Fig.2a

2.2 Characterization of Zn55Al coating

Fig.3a shows the surface morphology of the Zn55Al coating. It can be observed in Fig.3a that the Zn55Al coating is deposited on the Q235 substrate and that the surface is unsmooth, which is ascribed to the deposition process of the arc spray. The arc-sprayed wire becomes metal droplets and strikes the Q235 substrate at very high speeds because of the action of the arc and high-pressure gas. As a result, the larger-diameter Zn-Al metal droplets are also liquid before they contact the substrate. These larger-diameter particles achieve a sufficient deformation during spray atomization and have a high degree of flattening when they are deposited onto the metal surface of the substrate. On the other hand, the smaller-diameter metal droplets cool and transform to a semi-solid state before deposition on the substrate. The deformation ability of these semi-solid particles is worse than that of the liquid particles. Finally, these semi-solid alloys are attached to the surface to form protrusions.

The chemical composition of Zn55Al coating was tested by EDS and the data are shown in Table 2. The chemical content of Zn55 coating is similar to that of Zn55Al wire. The O element is found because of the oxide formed during the process of the arc spraying.

Fig.3b shows the cross-sectional morphology (BEI) of the Zn55Al coating. It shows that the coating exhibits an obvious lamellar structure with a few micro holes and gaps. The porosity of the Zn55Al coating is approximately 2.375%. It can be seen clearly that the lamellar structure is composed of layer phases that show different contrast in the BEI. Combining the elements distribution maps of Zn and Al, we know that the lighter phases are the Zn-rich phase and the darker phases are the Al-rich phase. The micro holes and gaps in the coating are also unavoidable due to the limitations of the arc-spraying method. The elements distribution maps of Zn and Al show that the chemical composition of the coating is substantially homogeneous over the whole cross-section.

The XRD pattern of the Zn55Al coating is presented in Fig.4. The Zn55Al coating is mainly composed of the Al-rich phase, Zn-rich phase and $Al_{0.403}Zn_{0.597}$ phase. Zn-rich phases and Al-rich phases are Zn solution and Al solution with alloying elements dissolving in their lattice. The Zn55Al pseudo-alloy wires melt to alloy liquid with different composition, and the alloy elements are not able to separate out owing to quick cooling. The diffraction peaks of the ZnO and Al_2O_3 phases are not detected by XRD analysis even though EDS detected the emission of oxygen element, indicating a slight oxidization during spraying.

It is concluded that the Zn55Al coating consists of the Zn-rich phases and Al-rich phases in a lamellar structure.

2.3 Corrosion behaviour of Zn55Al coating

Fig.5 shows the macroscopic corrosion morphology of the Zn55Al coating, Zn15Al coating and Al coating after 20 d immersion in 3.5 wt% NaCl solution at room temperature. Fig.5a and 5b shows the macroscopic corrosion morphologies of the Zn55Al coating and Zn15Al coating surfaces. An examination of Fig.5a and 5b clearly shows that the Zn55Al

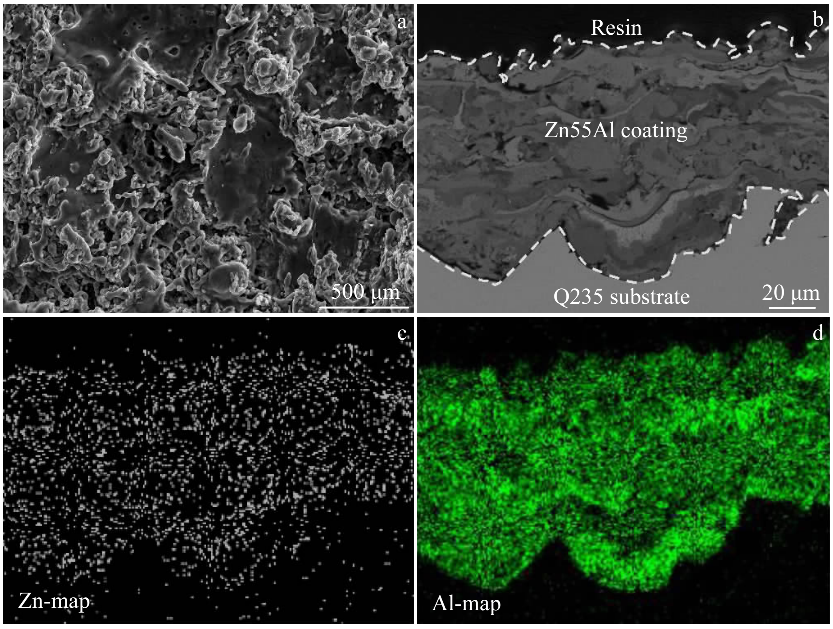

Fig.3 Surface (a) and cross-section (b) morphologies (BEI) of Zn55Al coating; distribution of Zn (c) and Al (d) elements

Table 2 Chemical composition of Zn55Al coating (wt%)

Zn	Al	O
44.03	51.82	4.15

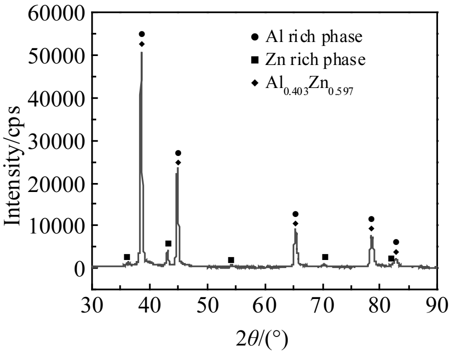

Fig.4 XRD pattern of the Zn55Al coating

coating and Zn15Al coating have generated a uniform corrosion products layer over the entire surface of coatings. The original coating cannot be seen at all. The corrosion product layer of Zn55Al coating is denser than that of Zn15Al coating. The corrosion products do not cover the whole Al coating surface and some red rust spots are found. The red rust spots are not found both on the Zn55Al coating and Zn15Al coating. The red rust spots show that the Q235 substrate has been corroded which means that the Al coating cannot provide the sufficient electrochemical production. So, the Zn55Al coating and Zn15Al coating exhibit better resistance to pitting corrosion than the pure Al coating.

Fig.6 shows the microscopic corrosion morphologies of the corrosion product layer and the cross-sectional corrosion morphologies of the Zn55Al coating and Zn15Al coating. According to Fig.6a, the corrosion products layer of Zn55Al coating consists of needle-like products, and the original morphology of the arc sprayed wire no longer exists. The needle-

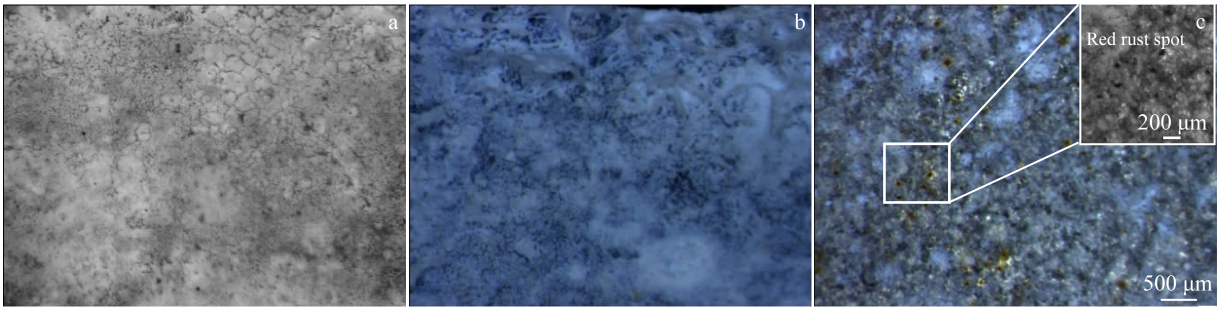

Fig.5 Macroscopic corrosion morphologies of the Zn55Al coating (a), Zn15Al coating (b), and Al coating (c) after 20 d immersion test in the 3.5 wt% NaCl solution at room temperature

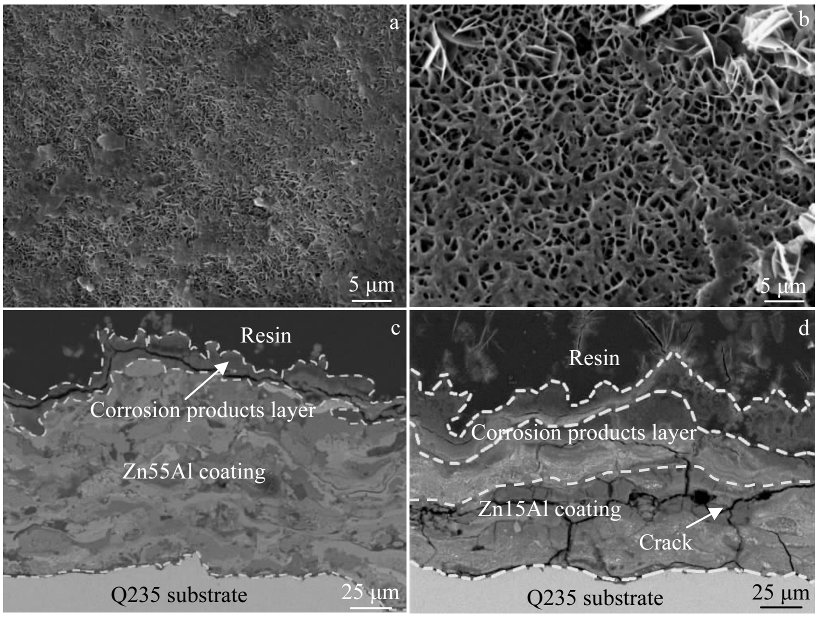

Fig.6 Microscopic corrosion morphologies of the corrosion product layer of Zn55Al (a) and Zn15Al coating (b); cross-sectional corrosion morphologies of Zn55Al (c) and Zn15Al coating (d) after 20 d immersion test in the 3.5 wt% NaCl solution at room temperature

like products grow and cross with each other to form a dense film during the immersion process. The micromorphology of the Zn15Al (Fig.6b) corrosion products has lots of holes which means that this corrosion products layer is looser than that of Zn55Al coating. This result coincides with the macroscopic corrosion morphology of the Zn55Al coating and Zn15Al coating. The denser corrosion products layer can prevent the corrosion medium from diffusion to the coating and thus decrease the corrosion rate of the coating.

Fig.6c and Fig.6d exhibit the cross-sectional microstructures of Zn55Al coating and Zn15Al coating after 20 d immersion corrosion test. After 20 d of the immersion corrosion test, the Zn55Al coating also shows good adhesivity with the Q235 substrate, and the lamellar structure is not destroyed. A dense oxide corrosion product layer has been generated on the surface of the Zn55Al coating. This dense corrosion product layer prevents the corrosion medium diffusing to the Zn55Al coating. Consequently, the Zn55Al coating shows an outstanding self-sealing behaviour. Thus, the Zn55Al coating can also provide good physical protection for the Q235 substrate after 20 d immersion test. After 20 d of immersion, a lot of cracks appear inside the Zn15Al coating, which destroy the layer structure of the original coating. The corrosion medium can easily contact the Q235 substrate through these cracks which accelerate the corrosion rate of the Zn15Al coating. So, it is clear that the corrosion resistance of Zn55Al coating is better than that of Zn15Al.

Fig.7 displays the phase composition of the corrosion products of the Zn55Al coating and Zn15Al coating analyzed by XRD. According to Fig.7a, the corrosion products of Zn55Al coating mainly contain $Zn_6Al_2(OH)_{16}CO_3\cdot4H_2O$, $Zn_{0.61}Al_{0.39}(OH)_2(CO_3)_{0.195}\cdot xH_2O$, $Zn_{0.63}Al_{0.37}(OH)_2(CO_3)_{0.185}\cdot xH_2O$, and $Al(OH)_3$ phases. However, the chloride cannot be found even when the immersion corrosion test was carried out in the NaCl solution. According to Fig.7b, the corrosion products of Zn15Al coating mainly contain $Zn_5(OH)_8Cl_2H_2O$, $Zn_{0.61}Al_{0.39}(OH)_2(CO_3)_{0.195}\cdot xH_2O$, and $Zn_{0.63}Al_{0.37}(OH)_2(CO_3)_{0.185}\cdot xH_2O$.

Comparing the XRD result of the corrosion products of Zn55Al coating (Fig.7a) with that of the Zn15Al coating (Fig.7b), it can be seen that $Al(OH)_3$ was only found in Zn55Al corrosion products, and $Zn_5(OH)_8Cl_2H_2O$ was only found in the Zn15Al corrosion products. Both the products of Zn55Al coating and Zn15Al coatings contain zinc aluminum carbonate hydroxide hydrate ($Zn_{0.61}Al_{0.39}(OH)_2(CO_3)_{0.195}\cdot xH_2O$, $Zn_{0.63}Al_{0.37}(OH)_2(CO_3)_{0.185}\cdot xH_2O$), which is formed by Zn^{2+}, Al^{3+}, OH^-, and CO_3^{2-}.

The formation of $Al(OH)_3$ can be described by Eqs. (1)~(4):

$$Al(s)\rightarrow Al^{3+}+3e^- \tag{1}$$

$$2Al^{3+}+3H_2O\rightarrow Al_2O_3+6H^+ \tag{2}$$

$$Al_2O_3+H_2O\rightarrow 2AlOOH \tag{3}$$

$$AlOOH+H_2O\rightarrow Al(OH)_3 \tag{4}$$

Liu's study indicates that the Al_2O_3 film is not stable in water and usually transforms into AlOOH or $Al(OH)_3$, which has higher stability than the Al_2O_3 film[24]. The Zn55Al coating could dissolve sufficient Al^{3+} to generate $Al(OH)_3$ films owing to its high Al content. The Zn15Al could also produce bits of the $Al(OH)_3$ products, but the $Al(OH)_3$ is not sufficient to form a dense film.

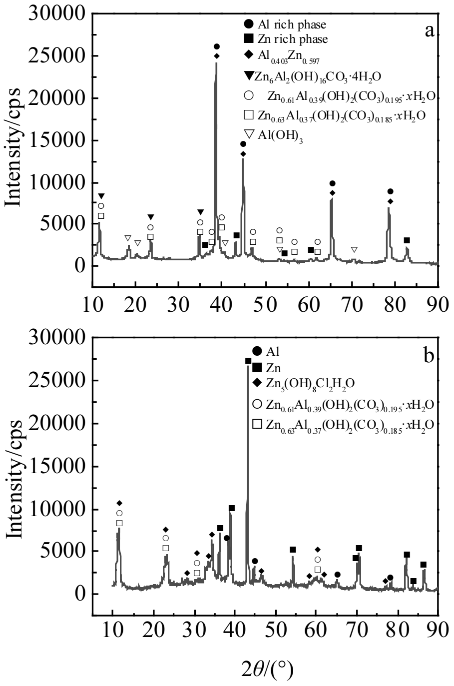

Fig.7 XRD patterns of the corrosion products of Zn55Al coating (a) and Zn15Al coating (b) after 20 d immersion test in the 3.5 wt% NaCl solution at room temperature

The formation of $Zn_5(OH)_8Cl_2H_2O$ is described by Eqs. (5)~(7).

$$Zn(s)\rightarrow Zn^{2+}+2e^- \tag{5}$$

$$Zn^{2+}+2OH^-\rightarrow Zn(OH)_2 \tag{6}$$

$$5Zn(OH)_2+H_2O+2Cl^-\rightarrow Zn_5(OH)_8Cl_2\cdot H_2O+2OH^- \tag{7}$$

Liu's study also indicates that the $Zn_5(OH)_8Cl_2H_2O$ does not show a strong bond to the coating owing to the ion-exchange mechanisms between the sheet structures[24]. The Zn15Al coating produces a high amount of $Zn_5(OH)_8Cl_2H_2O$, but the $Zn_5(OH)_8Cl_2H_2O$ could not form a dense film to seal the gaps and holes of the coating. Therefore, the corrosion products layer is looser than that of the Zn55Al coating.

We can conclude that the Zn55Al coating shows better corrosion resistance and self-sealing behaviour than the Zn15Al coating. This is due to the difference between the phase composition of the corrosion products.

2.4 Electrochemical measurements

Fig.8a shows the potentiodynamic polarization curves of the Zn55Al coating, Zn15Al coating and Al coating in 3.5 wt% NaCl solution. The corresponding electrochemical corrosion parameters derived from these polarization curves

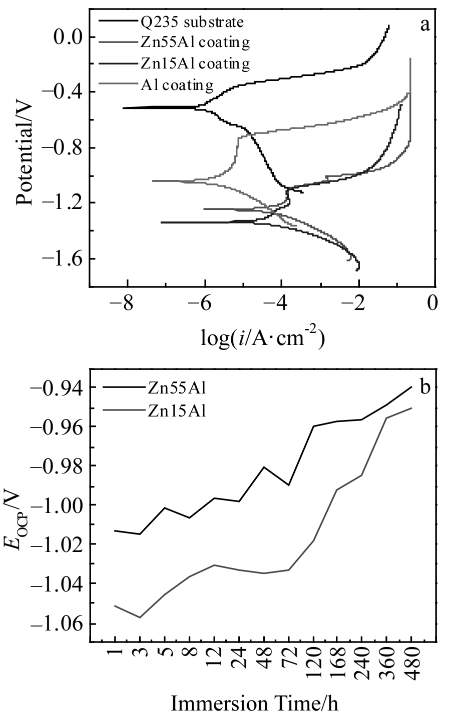

Fig.8 Potentiodynamic polarization curves of the three coatings and substrate (a); E_{OCP}-t curves of the Zn55Al coating and Zn15Al coating during the immersion corrosion test in the 3.5 wt% NaCl solution at room temperature (b)

are summarized in Table 3. The entire electrochemical test was repeated three times to obtain average values.

It is obvious from the results in Fig.8a and Table 3 that the corrosion potential of the three coatings is lower than that of the Q235 substrate. The Al coating has a more negative corrosion potential value than the Q235 substrate. However, the Al_2O_3 film formed by the Al coatings is more stable than the Fe substrate, and the Fe substrate will have a stronger tendency to become oxidized than the coatings. Hence, the spot corrosion phenomenon is very common in the Al coating corrosion process.

As shown in Fig.8a, the E_{corr} of the Zn55Al coatings is approximately −1.25 V. The E_{corr} of the Zn55Al coatings and Zn15Al coatings are more than 700 mV more negative than that of the Q235 substrate, so that the coatings can provide a sufficient driving force for cathodic protection to the substrate. The E_{corr} of the Zn55Al coatings is more positive than that of the Zn15Al coating, which means that the Zn55Al coating has a weaker corrosion tendency than Zn15Al coating in the dynamics theory. The i_{corr} of the Zn55Al coating is close to that of the Zn15Al coating.

Table 3 Electrochemical parameters obtained from polarization curves tested in 3.5 wt% NaCl solution at room temperature

Coating	E_{corr}/V	i_{corr}/×10^{-2} μA·cm^{-2}	R_p/Ω·cm^{-2}
Zn55Al	−1.246	5.76	464
Zn15Al	−1.329	5.46	520.2
Al	−1.082	0.641	14640.5
Fe	−0.512	0.881	17954.3

As shown in Fig.8a, the three coatings reveal a similar polarization behaviour character the distinct passive region in the anodic polarization. When the passivation film is broken, the current density increases sharply, indicating the initiation of pitting corrosion.

Fig.8b shows the variation of the open circuit potential (E_{OCP}) of the Zn55Al coating and Zn15Al coating with immersion time. For the entire test, the E_{OCP} of the Zn55Al coating is always higher than that of the Zn15Al coating. The E_{OCP} of Zn55Al and Zn15Al gradually increases with the immersion time owing to the formation of the passivation film and the accumulation of corrosion products[24]. The self- sealing behaviour caused by the corrosion products decreases the contact area between the coatings and the 3.5 wt% NaCl solution.

Fig.9 shows the result of the galvanic corrosion test. The E_g of Zn55Al coating is approximately 0.99 V and lower than that of Zn15Al coating which is about 1.03 V. The E_g shows that both coatings have electrochemical protection effect on the Q235 substrate but the Zn55Al coating has lower corrosion tendency than Zn15Al coating. This result coincides with the result of potentiodynamic polarization curves. The I_g of Zn55Al coating is about 29.1 μA and approximately 4 μA lower than that of Zn15Al coating after 3 h test. This result shows that Zn55Al coating has slower corrosion rate than Zn15Al coating.

In conclusion, the electrochemical test shows that Zn55Al can provide sufficient electrochemical protection.

2.5 Protective mechanisms of Zn55Al coating

In the present work, it is shown that Zn55Al coating has a better corrosion resistance than the Zn15Al coating and pure Al coating. According to the results described above, a schematic model of the protective machanisms of Zn55Al coating in NaCl solution is proposed in Fig.10.

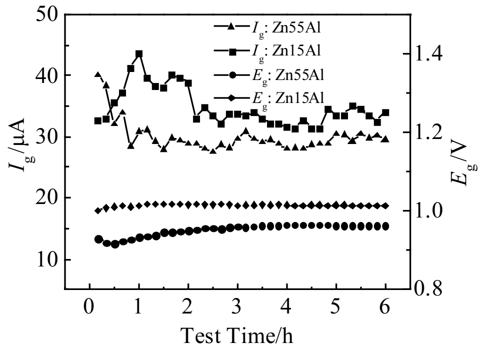

Fig.9 E_g and I_g of galvanic corrosion test between Zn-Al coating and Q235 substrate in 3.5 wt% NaCl solution at room temperature

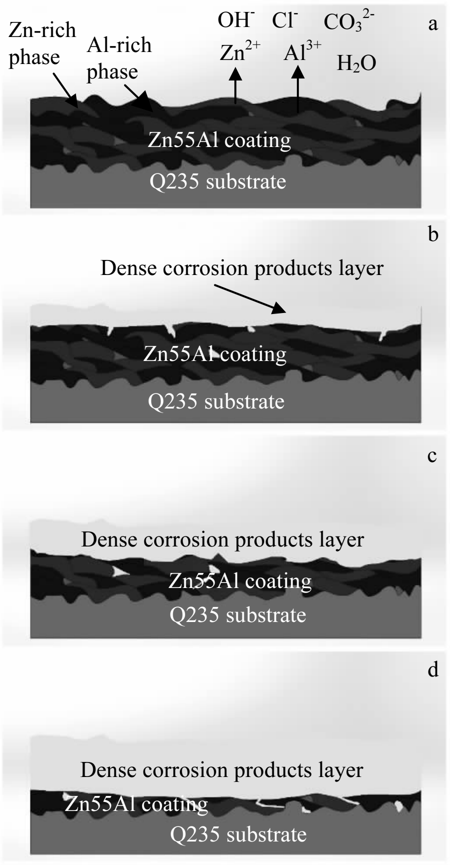

Fig.10 Schematic model of the protective mechanisms of Zn55Al coating in 3.5 wt% NaCl solution

The corrosion process can be divided into four steps. First, as shown in Fig.10a, the coating keeps the substrate from the corrosion medium though some holes and gaps existing in coating. Therefore, the corrosion medium only corrodes the surface and some holes near the surface of the coating. Zn^{2+} and Al^{3+} are dissolved from the coating and form corrosion products with OH^-, $CO_3^{2-}$and Cl^-.

Later, (Fig.10b), as the corrosion products are accumulated, a corrosion products layer is deposited on the coating surface. The Zn55Al coating is covered by a dense corrosion product layer completely. The self-healing behaviour occurs. The product layer and corrosion products decrease the contact area between the coating and corrosion medium, preventing the further corrosion of the coating.

As shown in Fig.10c, the corrosion medium continues corroding the coating over time. The thickness of the Zn55Al coating is gradually thinned. The physical protection decreases gradually.

Finally, the coating is not able to prevent the substrate from being completely affected by the corrosion medium (Fig.10d). Consequently, the coating and the substrate generate a primary battery system. The Zn55Al coating is the anode because its E_{corr} is lower than the Q235 substrate. In this term, Zn55Al coating can also provide good electrochemical protection to prevent the corrosion of the substrate.

In conclusion, Zn55Al can offer long-term protection owing to its self-sealing behaviour and the electrochemical protection.

3 Conclusions

1) The 3 mm Zn55Al pseudo-alloy wire was prepared by the multi-core canned hot extrusion and the cold drawing method. Alloying and eutectic structures are not found in the pseudo-alloy wire.

2) The Zn55Al coating was prepared by the arc-spraying method. The coating exhibits an obvious lamellar structure with a small number of holes and gaps. The microstructure of the coating is mainly composed of a Zn-rich phase, an Al-rich phase and $Al_{0.403}Zn_{0.597}$.

3) The corrosion products of the Zn55Al coating are denser than those of the Zn15Al coating, which means that the Zn55Al coating has a better self-sealing ability. The electrochemical test shows that Zn55Al coating can provide adequate electrochemical protection. Therefore, the Zn55Al coating possesses the greatest corrosion resistance among the three coatings.

References

1 Javaherdashti R. *Anti-Corrosion Methods and Materials*[J], 2000, 47(1): 30

2 González J A, Feliú S, Rodríguez P *et al. Materials & Structures*[J], 1996, 29: 40

3 Gyo J H, Yong Y J, Soo W J. *Transactions of the Iron & Steel Institute of Japan*[J], 2003, 43(10): 1603

4 Nishikata A, Zhu Q J, Tada E. *Corrosion Science*[J], 2014, 87: 80

5 Rocco A M, Nogueira T M C, Simão R A *et al. Surface and Coatings Technology*[J], 2004, 179(2-3): 135

6 Manna M, Naidu G, Rani N *et al. Surface and Coatings Technology*[J], 2008, 202(8): 1510

7 Yan D R, He J N, Tian B R *et al. Surface and Coatings Technology*[J], 2006, 201(6): 2662

8 Penney D J, Sullivan J H, Worsley D A. *Corrosion Science*[J], 2007, 49(3): 1321

9 Büteführ M. *Materials and Corrosion*[J], 2007, 58(9): 721

10 Xiao Y X, Jiang X H, Xiao Y D *et al. Procedia Engineering*[J], 2012, 27: 1644

11 Zhao W M, Wang Y, Liu C *et al. Surface and Coatings Technology*[J], 2010, 205(7): 2267

12 Kutz M. *Handbook of Environmental Degradation of Materials*[M]. New York: William Andrew, 2005: 405

13 Sugimura S, Liao J S. *Surface and Coatings Technology*[J], 2016, 302: 398

14 Yang H Q, Yao Z J, Wei D B *et al. Surface Engineering*[J], 2014, 30(11): 801

15 Chen Y X, Liu Y, Liang X B *et al. Journal of Materials Engineering*[J], 2009, 3: 65 (in Chinese)

16 Jiang Q, Miao Q, Liang W P *et al*. *Electrochimica Acta*[J], 2014, 115: 644

17 Jiang Q, Miao Q, Tong F *et al*. *Transactions of Nonferrous Metals Society of China*[J], 2014, 24(8): 2713

18 Yang L J, Zhang Y M, Zeng X D *et al*. *Corrosion Science*[J], 2012, 59: 229

19 Panossian Z, Mariaca L, Morcillo M *et al*. *Surface and Coatings Technology*[J], 2005, 190(2-3): 244

20 Liu Y, Zhu Z X, Chen Y X *et al*. *Transactions of Nonferrous Metals Society of China*[J], 2004, 14(S1): 443

21 Zhang C W, Zhou L, Sulpice A *et al*. *Science China Technological Sciences*[J], 2010, 53(11): 3020

22 Wu X, Peng X, Sumption M D *et al*. *IEEE Transactions on Applied Superconductivity*[J], 2005, 15(2): 3399

23 Sumption M D, Peng X, Lee E *et al*. *Cryogenics*[J], 2004, 44(10): 711

24 Liu Y, Li H Y, Li Z G. *International Journal of Electrochemical Science*[J], 2013, 8(6): 7753

Q235 上电弧喷涂 Zn55Al 涂层在 3.5%NaCl 溶液中的腐蚀行为

冯上宾，贾丽娜，张花蕊，王方方，刘光旭，张　虎
(北京航空航天大学，北京 100191)

摘　要：使用电弧喷涂通过包套挤压+拉拔的方法制备的 Zn55Al 伪合金丝材在 Q235 钢上喷涂出了 Zn55Al 涂层。通过扫描电镜和微区 XRD 研究了 Zn55Al 伪合金丝材的显微结构。通过浸泡腐蚀实验和电化学方法研究了 Zn55Al 涂层、Zn15Al 涂层和 Al 涂层的腐蚀行为，并对比了 3 种涂层之间的差异。结果表明 Zn55Al 伪合金丝材由纯锌和纯铝组成，在整个成型过程中没有产生合金化。Zn55Al 涂层由层片状的富锌相和富铝相组成。经过 20 d 的浸泡实验，Zn55Al 涂层形成了一层致密的钝化膜，比其他 2 种涂层有更好的耐腐蚀性。Zn55Al 涂层的自腐蚀电位大约是–1.25 V，高于 Zn15Al 涂层，低于纯 Al 涂层和 Q235 基体。电偶腐蚀实验表明，Zn55Al 涂层比 Zn15Al 涂层具有更好的电化学保护作用。这些结果说明 Zn55Al 涂层具有更好的耐腐蚀性，可以给 Q235 基体提供更强的电化学保护。本研究也讨论了 Zn55Al 涂层的的腐蚀机理。

关键词：多芯包套热挤压；Zn55Al 伪合金丝；Zn55Al 涂层；腐蚀行为

作者简介：冯上宾，男，1992 年生，硕士生，北京航空航天大学材料科学与工程学院，北京 100191，电话：010-82339256，E-mail: shangbin@buaa.edu.cn